Gaussian Pulse Propagation in Dispersion-Managed Systems Using Chirped Fiber Gratings With Group Delay Ripples

Y. H. C. Kwan, K. Nakkeeran, P. K. A. Wai, *Senior Member, IEEE*, and P. Tchofo Dinda

***Abstract*—We study the propagation of Gaussian-shaped pulses in grating-compensated dispersion-managed systems with group delay ripples (GDR). We show that the intersymbol interference caused by the GDR in gratings can be substantially reduced by nonlinear optical loop mirrors and the 40-Gb/s system performance can achieve transoceanic transmission in the presence of amplifier noise and random variations in ripple period of the gratings along the transmission line.**

***Index Terms*—Dispersion-managed (DM) systems, gratings, group delay ripples (GDR), nonlinear optical loop mirrors (NOLMs), optical communications.**

I. Introduction

DISPERSION management is a key element in high-speed long-haul optical communication systems, which exploits various types of dispersion compensating techniques. One of the commonly used techniques lies in dispersion compensating fibers (DCFs). Another important technique lies in the use of chirped fiber gratings (CFGs), in which the typical length of the CFG for compensating 100 km of single-mode fiber (SMF) is only $\sim$20 cm. The CFGs can also compensate the dispersion at orders higher than the second order, and have low insertion loss. It has been shown that solitons exist in dispersion-managed (DM) systems utilizing CFGs for dispersion compensation [1], [2]. Experiments have been carried out at 10 Gb/s over 2900 km [3] and 40 Gb/s over 500 km [4] utilizing CFGs for dispersion compensation.

The major constraint in using CFGs for dispersion compensation is the group delay ripples (GDR) which are caused by the imperfections in grating manufacturing processes [5]. The GDR introduces side peaks in the pulse profile, as shown in Fig. 1, and leads to intersymbol interference (ISI). In linear systems, the amplitude of these side peaks grows linearly with the number of CFGs along the propagation distance [6]. We have shown that soliton transmission, unlike in linear systems, can substantially suppress the growth of these side peaks [2]. In most practical situations, the side peaks are still present and may cause ISI. Different grating fabricating methods were proposed to eliminate the GDR, but GDR remains [5]. It was demonstrated that nonlinear optical loop mirror (NOLM) can be utilized for 2R regeneration in return-to-zero DM transmission system using DCFs [7], [8]. We have shown that NOLMs can also be used to significantly reduce the side peaks in lossless [9] and in lossy grating-compensated DM soliton systems [10].

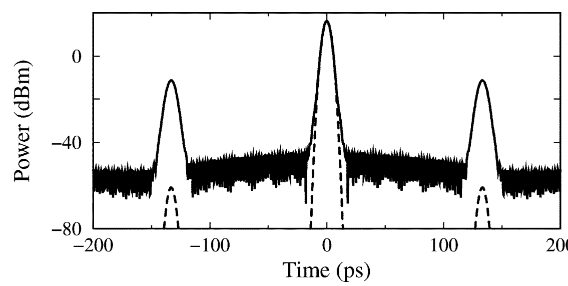

Fig. 1. Temporal shapes of the single pulse having the same energy and width in the DM fiber system without NOLMs (solid) and with NOLMs (dashed).

In this work, we show that the use of NOLMs can effectively reduce the amplitudes of the side peaks in lossy grating-compensated DM communication systems using Gaussian pulses at high speeds, such as 40 Gb/s. Generation of Gaussian-shaped pulses by means of standard laser sources is much easier than the generation of DM solitons. To model the practical system, we have included the amplifier noise in the transmission line. We have found that the transmission performance depends on the location of first side peaks (the nearest neighbors of the central peak) [10]. In addition, it is impossible to fabricate gratings having the same structure of GDR. Thus, we consider random variations in the ripple period of the CFGs along the propagation distance. We compare the system performance without and with NOLMs and find that the appropriate use of in-line NOLMs enables an error-free transoceanic transmission.

II. System Modeling

The dynamics of a pulse propagating in an optical fiber under the influence of the Kerr nonlinearity and varying dispersion is governed by the nonlinear Schrödinger (NLS) equation

$$i\frac{\partial q}{\partial z} - \left[\frac{\beta(z)}{2}\right]\frac{\partial^2 q}{\partial t^2} + \gamma|q|^2 q = 0$$

where q is the slowly varying envelope of the axial electrical field, $\beta(z)$ and γ represent the group velocity dispersion (GVD) and self-phase modulation parameters, respectively.

Manuscript received November 2, 2004; revised January 12, 2005. This work was supported in part by the Research Grant Council of the Hong Kong Special Administrative Region, China, under Project PolyU5242/03E. The work of P. Tchofo Dinda was supported by The Hong Kong Polytechnic University for hospitality.

Y. H. C. Kwan, K. Nakkeeran, and P. K. A. Wai are with the Photonics Research Centre and Department of Electronic and Information Engineering, The Hong Kong Polytechnic University, Hung Hom, Hong Kong (e-mail: canny@eie.polyu.edu.hk).

P. Tchofo Dinda is with the Laboratoire de Physique de l'Université de Bourgogne, Dijon 21078, France.

Digital Object Identifier 10.1109/LPT.2005.845778

In this study, the minimum pulsewidth is about 5 ps. We, thus, neglect the higher order dispersion and nonlinear effects in the systems. The GVD parameter $\beta(z) = \beta$ for $z \neq (n+1/2)L$, where n is an integer and L is the dispersion map length. The gratings are located at $z = (n+1/2)L$ and their actions are given by the transfer function $F(\omega)$ such that $Q_{\text{out}}(z,\omega) = F(\omega)Q_{\text{in}}(z,\omega)$, where ω is the angular frequency, Q_{in} and Q_{out} are the pulse spectra before and after the gratings. The complex GDR structure can be obtained by solving the coupled-mode equations [11]. In [9], we used the coupled-mode equations to model the CFG and found that the side peaks suppression using NOLMs is much stronger than that using sinusoidal function for modeling GDR. Here, for simplicity, we consider a lossless grating, which induces a strong flat-top reflectivity. The bandwidth of the grating is assumed to be much greater than the signal bandwidth, and the ripples have sinusoidal profiles [2]. Mathematically, the transfer function of the grating is given by

$$F(\omega) = \exp\left[i\frac{g}{2}\omega^2 - i\frac{\Gamma}{T_0^2}\cos(\omega T_0 + \theta) + i\frac{\Gamma}{T_0^2}\right]$$

where g is the average lumped dispersion of the grating and the average system dispersion $\bar{\beta} = (\beta L + g)/L$. The parameters Γ, $2\pi/T_0$, and θ are the amplitude, period, and phase of the grating dispersion ripples, respectively. The lumped dispersion of the grating is, therefore, given by $g + \Gamma\cos(\omega T_0 + \theta)$.

III. Numerical Results

We consider a DM system that consists of fiber segments and CFGs. The CFG is located at the middle of the dispersion map. The dispersion map is designed using an analytical method [12], with map strength of 1.65 that minimizes the pulse–pulse interactions. The fiber has a dispersion of 1.62 ps/nm/km, nonlinearity of 2 $\text{km}^{-1}\text{W}^{-1}$, and loss coefficient of 0.2 dB/km. We use a different transmission fiber (not SMF) in order to obtain a longer dispersion map length for the same map strength. We choose the pulse energy of 0.23 pJ and width of 5 ps for simulating a 40-Gb/s system. Using these fiber and pulse parameters in the analytical method [12], we have designed a dispersion map having fiber segment of length $\sim$10.28 km and grating dispersion of -15.6 ps/nm. Thus, the average dispersion is 0.11 ps/nm/km. It is worth noting that if we use a DCF (-90 ps/nm/km), the required length would be $\sim$173 m, which is much more bulky than the equivalent CFG (only $\sim$20 mm long). The GDR in CFGs has an amplitude of 3 ps, a period of 0.06 nm, and a phase of π. In [13], it has been reported that the ripple amplitude can be as low as 1.5 ps and a dominant period is 0.06 nm. We study the cases of fixed and random variation in the GDR ripple period of the CFGs along the transmission line. The amplifier spacing is four times the dispersion map length.

An NOLM is placed after each amplifier and the schematic is shown in Fig. 2. The NOLM consists of a 50 : 50 coupler, a dispersion-shifted fiber with length of 90.3 m, zero dispersion, nonlinearity of 4 $\text{km}^{-1}\text{W}^{-1}$, and loss coefficient of 0.3 dB/km. We use an attenuator (22.4 dB) to break the symmetry, a filter (bandwidth 110.3 GHz) to reshape the pulse, and a loss element (0.46 dB) after the loop to balance between the input and output pulse powers in the NOLMs. The amplifier in the system with the NOLMs has a gain of 35.2 dB, which compensates both the power loss in the in-line fiber and the NOLM and the NOLM can operate at an input pulse peak power of 21.6 W.

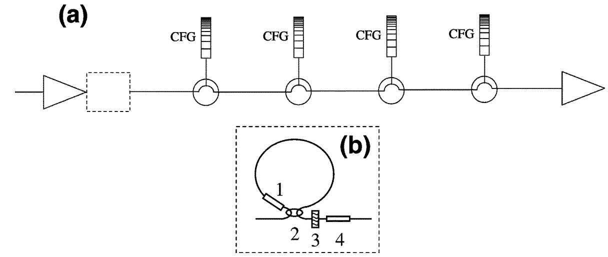

Fig. 2. (a) Schematic of the transmission system and the dashed box is shown in (b) the configuration of the NOLMs. (1) and (4) Attenuators. (2) 50 : 50 coupler. (3) Filter.

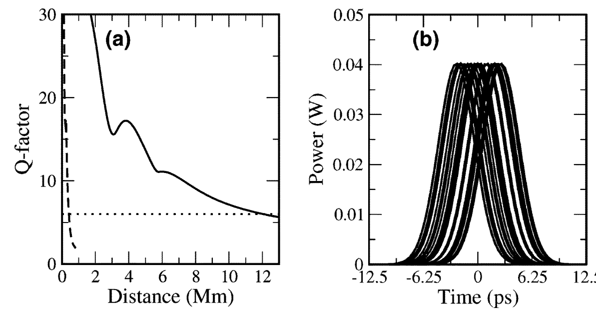

Fig. 3. (a) Q-factors in the system without (dashed curve) and with (solid curve) NOLMs. (b) The corresponding eye diagram in the system with NOLMs at 12 Mm. The system has no amplifier noise.

A. Fixed Ripple Period

Fig. 1 shows the stable solution in the system without (solid) and with NOLMs (dashed) and the first side peaks are suppressed about 50 dB. The NOLM acts as a nonlinear intensity filter which will enhance the pulse peak power. The parts of the pulse profile which are much smaller than the peak power are strongly attenuated when passing through the NOLM, hence, the suppression of the pedestals containing the side peaks. We find that the NOLMs converge the initial Gaussian pulse quickly into a stable solution. The pulse profile is taken after the amplifiers and NOLMs in the system without and with NOLMs and the corresponding pulsewidths are 5.04 and 4.91 ps, respectively.

To illustrate the effectiveness of NOLMs, we launch a 128-bit Gaussian-shaped sequence with mark ratio of 0.5 and bit window of 25 ps in the system and use gratings with fixed period for GDR (0.06 nm). We examine the transmission performance by solving the NLS equation. Fig. 3(a) shows the Q-factors of the transmission performance without (dashed) and with (solid) NOLMs in the systems. The dotted line represents $Q = 6$ which corresponds to a bit-error rate of 10^{-9}. The eye diagram at 12 Mm in the case with NOLMs is shown in Fig. 3(b). We find the error-free transmission distance in the system with neither GDR nor NOLMs is $\sim$10.9 Mm. Thus, the degradation of the transmission performance in the system without NOLMs is mainly caused by the GDR [dashed curve in Fig. 3(a)]. It shows that the NOLMs can significantly reduce the effect of GDR. The large improvement in the transmission performance is due to the side peaks suppression by NOLMs. On the other hand, we have performed numerical simulations

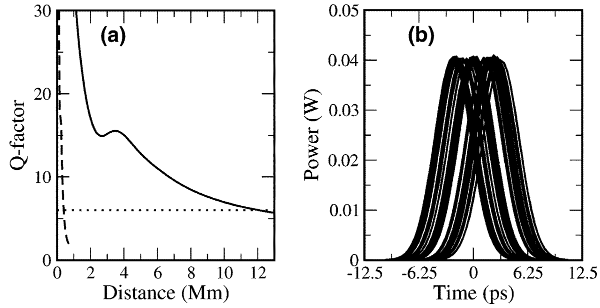

Fig. 4. (a) Q-factors in the system without (dashed curve) and with (solid curve) NOLMs. (b) The corresponding eye diagram in the system with NOLMs at 12.1 Mm. The system includes amplifier noise.

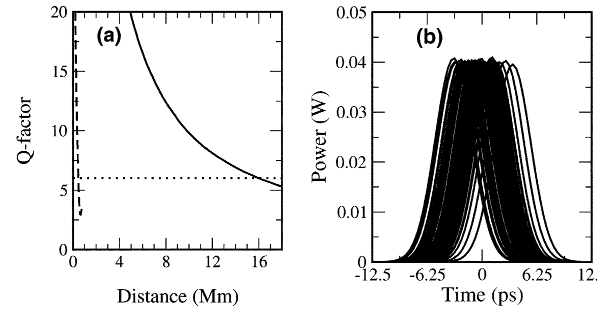

Fig. 5. (a) Q-factors in the system without (dashed curve) and with (solid curve) NOLMs. (b) The corresponding eye diagram in the system with NOLMs at 16.1 Mm. The system includes amplifier noise and changing the ripple period in the gratings along the transmission.

not presented here, with the loop length of the NOLM increased by 5%, and found that the error-free transmission distance is still 12 Mm. This indicates that the system is quite tolerant to slight variations in the NOLM parameters.

For practical study, we include the amplifier noise with noise figure of 4.5 dB in the system. The Q-factors of the transmission performance without (dashed) and with (solid) NOLMs in the system are shown in Fig. 4(a). We use 50 realizations in bit sequence and noise to calculate the Q-factors. The error-free transmission distances without and with NOLMs are 0.37 and 12.1 Mm, respectively. Fig. 4(b) shows the corresponding eye diagram of a pulse sequence with NOLMs at 12.1 Mm. Thus, the NOLMs stabilize the pulse peak power. The results show that the amplitude of side peaks and the amplifier noise can be simultaneously reduced using NOLMs.

B. Random Variations in the Ripple Period

The separation between the pulse peaks (see Fig. 1) is inversely related to the ripple period and we find that the location of first side peaks affects the transmission performance [10]. In this study, the ripple period of CFGs is randomly varied along the transmission distance and in the grating spectrum with a normal distribution fashion having a mean of 0.06 nm (7.5 GHz) and standard deviation of 0.0056 nm (0.7 GHz). This provides 68% probability of ripple period to lie in the range between 0.0544 (6.8 GHz) and 0.0656 nm (8.2 GHz) which gives a side peaks separation varying between 122 and 147 ps. Thus, the location of the first side peaks will be having a 68% chance of variation within a bit slot (25 ps) around the mean period (0.06 nm). The amplitude and phase of the GDR are fixed to be 3 ps and π, respectively.

The pulse and system parameters are the same as in the case of fixed ripple period study. Here also we launch 128-bit Gaussian-shaped pseudorandom sequence with amplifier noise into the system. Fig. 5(a) shows the Q-factors of the transmission performance without (dashed) and with (solid) NOLMs in the system. The eye diagram with NOLMs in the system at 16.1 Mm is shown in Fig. 5(b). It demonstrates that the use of NOLMs can significantly reduce the effect of GDR even in the case of random variation in the GDR ripple period of the CFGs along the transmission line with amplifier noise.

IV. Conclusion

We have shown that the use of NOLMs can substantially improve the transmission performance in the grating-compensated DM fiber systems with GDR in CFGs. The error-free transmission can achieve transoceanic distance even with amplifier noise and random variation of ripple period in CFGs along the propagation distance.

References

[1] S. K. Turitsyn and V. K. Mezentsev, "Chirped solitons with strong confinement in transmission links with in-line fiber Bragg gratings," *Opt. Lett.*, vol. 23, pp. 600–602, 1998.

[2] Y. H. C. Kwan, P. K. A. Wai, and H. Y. Tam, "Effect of group-delay ripples on dispersion-managed soliton communication systems with chirped fiber gratings," *Opt. Lett.*, vol. 26, pp. 959–961, 2001.

[3] E. Yamada, T. Imai, T. Komukai, and M. Nakazawa, "10 Gbit/s soliton transmission over 2900 km using 1.3 μm singlemode fibers and dispersion compensation using chirped fiber Bragg gratings," *Electron. Lett.*, vol. 35, pp. 728–729, 1999.

[4] A. Sahara, T. Komukai, E. Yamada, and M. Nakazawa, "40 Gbit/s return-to-zero transmission over 500 km of standard fibre using chirped fibre Bragg gratings with small group delay ripples," *Electron. Lett.*, vol. 37, pp. 8–9, 2001.

[5] T. Komukai, T. Inui, and M. Nakazawa, "Origin of group delay ripple in chirped fiber Bragg gratings and its effective reduction method," *Electron. Commun. Jpn.*, pt. 2, vol. 86, pp. 76–84, 2003.

[6] S. G. Evangelides, N. S. Bergano, and C. R. Davidson, "Intersymbol interference induced by delay ripple in fiber Bragg gratings," in *Proc. OFC Conf.*, vol. 4, San Diego, CA, Feb. 21–26, 1999, pp. 5–7.

[7] S. Boscolo, S. K. Turitsyn, and K. J. Blow, "All-optical passive 2R regeneration for N × 40 Gbit/s WDM transmission using NOLM and novel filtering technique," *Opt. Commun.*, vol. 217, pp. 227–232, 2003.

[8] F. Seguineau, B. Lavigne, D. Rouvillain, P. Brindel, L. Pierre, and O. Leclerc, "Experiment demonstration of simple NOLM-based 2R regenerator for 42.66 Gbit/s WDM long-haul transmissions," in *Proc. OFC Conf.*, Los Angeles, CA, Feb. 22–27, 2004, Paper WN4.

[9] Y. H. C. Kwan, K. Nakkeeran, and P. K. A. Wai, "Reduction of intersymbol interference in dispersion-managed soliton systems compensated by chirped fiber gratings," in *Proc. Pacific Rim Conf. Lasers and Electro-Optics (CLEO/PR)*, vol. 1, Taiwan, Dec. 15–19, 2003, Paper W1F-(5)-3.

[10] Y. H. C. Kwan, K. Nakkeeran, P. K. A. Wai, and P. Tchofo Dinda, "Significant improvement of performance in grating-compensated transmission systems using nonlinear optical loop mirrors," in *Proc. Int. Conf. Optical Communications and Networks (ICOCN)*, Hong Kong, 30 Nov.–1 Dec. 2004, pp. 39–42.

[11] R. Kashyap, *Fiber Bragg Gratings*. New York: Academic, 1999, ch. 4.

[12] Y. H. C. Kwan, K. Nakkeeran, and P. K. A. Wai, "Analytical method for designing grating compensated dispersion-managed soliton systems," *J. Opt. Soc. Amer. B*, vol. 21, pp. 706–718, 2004.

[13] H. Chotard, Y. Painchaud, A. Mailloux, M. Morin, F. Trépanier, and M. Guy, "Group delay ripple of cascaded Bragg grating gain flattening filters," *IEEE Photon. Technol. Lett.*, vol. 14, no. 8, pp. 1130–1132, Aug. 2002.